Investigation of large scale flow structures in an offset attaching jet using spectral linear stochastic estimation

Nan Gao

School of Aeronautics and Astronautics, Dalian University of Technology, Dalian, China

Dan Ewing

Toronto, Canada

The large scale flow structures in an offset attaching jet with an offset height equal to the jet height and $Re = 44\,000$ were studied using simultaneous measurements of the fluctuating wall pressure along the streamwise direction and the fluctuating velocity field estimated using a spectral linear stochastic estimation (LSE) technique. Box filters were used to examine the flow structures with different characteristic frequencies. The results showed evidence of different dominant flow structures in the flow. The instantaneous distributions of the estimated velocities and vorticity were examined for periods when different modes were prominent and showed differences in the behavior of the flow structures in the flow.

I. Introduction

Offset jets with modest offset distances are used in a range of different cooling applications. The offset jets produce a local maximum in the heat transfer where they attached to the wall. The magnitude of the heat transfer at this point decreases as the offset distance of the jet (H_s) increases even for jets with $H_s/H_j \leq 1$ despite an increase in the turbulence level in the flow near this point. This suggest there may be a change in the way the flow structures interact with the wall as H_s changes even for $H_s/H_j \leq 1$. Recently, Gao and Ewing[4] studied the flow structures in offset attaching jet with $H_s/H_j \leq 1$ using the correlation between the fluctuating wall pressure and the fluctuating velocities, and found features near the reattachment point similar to other reattaching shear layer flows such as flow over a backward facing step or flow separated from a bluff body.[2,9,10] In particular, there were shedding mode motions with a frequency of $fX_r/U_j \approx 0.5$ to 1 and a low frequency flapping instability with $fX_r/U_j < 0.2$. Here, X_r is the mean reattachment length. The structures formed in the inner shear layer then developed downstream and appeared to merge with the structures in the outer shear layer of the jet. The outer shear layer structures grew in size while the jet was attaching to the wall and eventually became similar to the structures in a planar wall jet with a frequency $fH_j/U_j < 0.1$.

Gao and Ewing[5] studied the coherence of the fluctuating pressure and velocity in an offset jet with $H_s/H_j = 1$ and the propagation velocity of the structures in this flow by considering the change in the phase of the cross-spectra of the fluctuating pressure along the wall and the cross-spectra of the fluctuating wall pressure and fluctuating velocity throughout the flow. They found that the propagation speed of these motions varied with frequency. In particular, they found evidence of two modes in the inner shear layer, $0.6 \lesssim fX_r/U_j \lesssim 0.9$ and $0.9 \lesssim fX_r/U_j \lesssim 1.4$, that had different propagation velocities. They also found evidence that motions with $0.3 \lesssim fX_r/U_j \lesssim 0.6$ propagated downstream slower than the higher frequency motions. These slower motions appear to be associated with the structures that eventually form the wall jet structures travelled slower than the inner shear layer structures. The propagation velocity for the motions with $fX_r/U_j < 0.3$ varied linearly with frequency and was consistent with a flapping motion.

The objective of this investigation was to examine if the dynamics and interactions of different structures can be captured in the instantaneous fluctuating velocities estimated using a spectral linear stochastic estimation technique.[3] In this approach, the instantaneous velocity field is estimated from simultaneous time resolved measurements of the fluctuating wall pressure using coefficients that depend on the pressure velocity cross-spectra. Tinney et al.[12] and Hall and Ewing[6] found that the spectral LSE produced better estimations

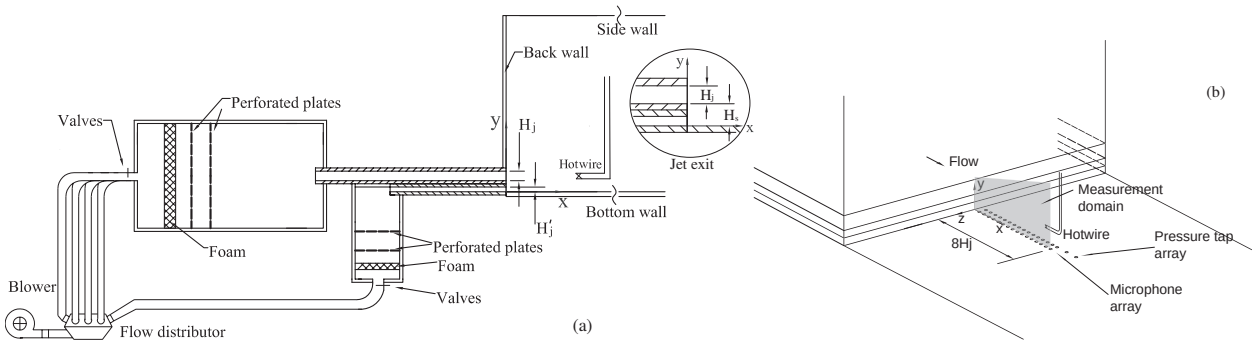

Figure 1. Schematics of (a) the offset attaching jet facility with an offset distance $H_s/H_j = 1.0$ and (b) the plan of the flow measurements.

than a single time LSE technique, particularly in the flows with convected flow structures. The analysis here uses the data presented in Gao and Ewing.[4,5] The experimental facility and analysis methodology used in this investigation are outlined in the next section. The preliminary results are then presented and discussed.

II. Experimental Methodology

The measurements reported in Gao and Ewing[4,5] were performed in the facility shown in Fig. 1(a). The jet exits a channel with a height (H_j) of 3.8cm and a length of 81 cm or $22H_j$. The width of the channel and the facility (W) was 74.3 cm or 19.5 H_j. Flow supplied by a variable speed blower entered a settling chamber (122cm by 72.4cm by 45.7cm) and was conditioned using flow straightening sections and screens before entering the square edged reentrant entrance of the channel. The facility had a second lower channel as shown in Fig. 1(a) but the exit of this channel was blocked. The measurements were performed for an average outlet velocity (U_j) of 18.4 m/s that corresponded to a Reynolds number based on jet height of approximately 44 000. The profiles of the mean velocity and turbulent stresses measured at the exit of the channel for a free jet were symmetric and fully developed. The flow exiting the channel developed over a 180 cm long plate mounted parallel to the channel at a distance (H_s) of 3.8 *cm* (or H_j) below the bottom of the channel, and between 100 cm high side walls. The boundary layers on the side walls were to approximately $5H_j$ at $x/H_j = 12$.

The fluctuating pressure on the wall below the attaching jet was measured using an array of 16 microphones that have flat responses for 20Hz to 5000Hz. The microphones were mounted into blind cavities drilled from the bottom of the wall. The microphones were positioned from x/H_j= 0.5 to 8 with a streamwise spacing of $0.5H_j$, as shown in Fig. 1(b). The microphones sensed the flow through 1.6mm-diameter, 5mm-long pinholes drilled through the wall to the top of the cavity. The microphones were calibrated externally with a piston phone at 1000Hz. The spectra of the fluctuating wall pressure measured through the pinholes agreed with the results for a flush mounted microphones for frequencies up to 400Hz.

The flow velocity was measured using a cross hot-wire probe with an in-house anemometry system. The probe was calibrated in a separate facility and the response curves for the individual wires were fit with four-order polynomials, while the response of the cross-wire was fit using a modified cosine law.[1] The probe was moved using a computer controlled traverse that could be positioned with an accuracy less than 0.05mm. Rectification affected approximately 2.5% of the data points at the inner half-width of the attaching shear layer. The output signals from the microphones and hot-wire anemometers were sampled simultaneously at a frequency of 2048Hz for 150 independent blocks of 1024 data points. The uncertainty in the velocity and pressure spectra were ±8% at the 95% confidence interval. The measurements in the velocity field were performed on a point by point basis. Thus, there were not simultaneous measurements of the velocities in the field (though there were simultaneous measurements of the fluctuating pressure along the wall).

A. Spectral LSE

Realizations of fluctuating streamwise and vertical velocities were estimated using a spectral linear stochastic estimation technique.[3,6,12] In this approach, the Fourier coefficient of the velocity components at each

location $\hat{u}_e(x_\alpha, y, f)$ and $\hat{v}_e(x_\alpha, y, f)$ are estimated using

$$\hat{u}_e(x_\alpha, y, f) = \sum_{\beta=1}^{N} A_\beta(x_\alpha, y, f)\hat{p}(x_\beta, f), \tag{1}$$

$$\hat{v}_e(x_\alpha, y, f) = \sum_{\beta=1}^{N} B_\beta(x_\alpha, y, f)\hat{p}(x_\beta, f), \tag{2}$$

where $\hat{p}(x_\beta, f)$ is the Fourier coefficient of the fluctuating wall pressure, N is the total number of microphones. The matrix of the estimation coefficients $A_\beta(x_\alpha, y, f)$ and $B_\beta(x_\alpha, y, f)$ were determined by minimizing the mean square error in the spectra computed from the estimated Fourier coefficients. The matrix of estimation coefficients $A_\beta(x_\alpha, y, f)$ and $B_\beta(x_\alpha, y, f)$ are the solutions of the linear equations, given by

$$F_{up}(x_\alpha, x_\beta, y, f) = \sum_{\beta=1}^{N} A_\beta(x_\alpha, y, f)F_{pp}(x_\alpha, x_\beta, f), \tag{3}$$

$$F_{vp}(x_\alpha, x_\beta, y, f) = \sum_{\beta=1}^{N} B_\beta(x_\alpha, y, f)F_{pp}(x_\alpha, x_\beta, f), \tag{4}$$

where there are a set of N equations (in β) at each frequency. The estimation process was performed using discrete spectra. Thus the spectra and the cross spectra for different locations are given by

$$F_{pp}(x_\alpha, x_\beta, f) = \frac{\overline{\hat{p}(x_\alpha, f)\hat{p}^*(x_\beta, f)}}{T}, \tag{5}$$

$$F_{up}(x_\alpha, x_\beta, y, f) = \frac{\overline{\hat{u}(x_\alpha, y, f)\hat{p}^*(x_\beta, f)}}{T}, \tag{6}$$

and

$$F_{vp}(x_\alpha, x_\beta, y, f) = \frac{\overline{\hat{v}(x_\alpha, y, f)\hat{p}^*(x_\beta, f)}}{T}. \tag{7}$$

Here, $\hat{u}(x_\alpha, y, f)$ and $\hat{v}(x_\alpha, y, f)$ are the Fourier coefficients of the fluctuating streamwise and vertical velocities determined in the point by point measurements, * is the complex conjugate, and T is the length of each data block. The estimated Fourier coefficients at all points can then be computed from equation (1) and (2) using any block of the simultaneous pressure measurements. The estimated velocities are then determined by the inverse Fourier transforming the estimated coefficients.

III. Results and Discussions

The development of the mean flow field and the actual and estimated fluctuating velocities are shown in Fig. 2. The offset jet approached the wall and then attached to the wall in a mean sense at $X_r \approx 4.6H_j$. Measurements in the jets with a range of offset jet with $H_s/H_j \leq 1.0$ showed that the development of the mean flow can be divided into 5 regions.[4] The maximum mean velocity was approximately constant in Region I ($x/X_r \leq 0.65$) before the maximum velocity decreased as the jet attached to the wall in Region II ($0.65 < x/X_r \leq 1.1$). The attaching jet recovered downstream of the reattachment point in Region III with an approximately constant maximum mean velocity before this velocity decreased as the flow transitioned to a wall jet flow in Region IV ($6 \lesssim x/H_j \lesssim 10$) and then became similar to a fully developed planar wall jet flow in Region V ($x/H_j \geq 10$). The magnitude of the fluctuating velocity grew as the shear layer on either side of the jet developed. The vertical fluctuating velocities were larger in the inner shear layer above the recirculating flow region. The fluctuations in the inner shear layer reached a maximum where the jet attached to the wall as the shear layer interacted with the wall. The fluctuations in the outer layer continued to increase in magnitude as the flow evolved downstream and became larger than the inner fluctuations in the wall jet region. The rms values of the estimated velocities were less than the measured velocities. The maxima in u'_e and v'_e occurred at the same vertical locations in the profiles of u' and v' indicating the estimation process captured the location of the shear layers. The maxima of the rms values for the estimated

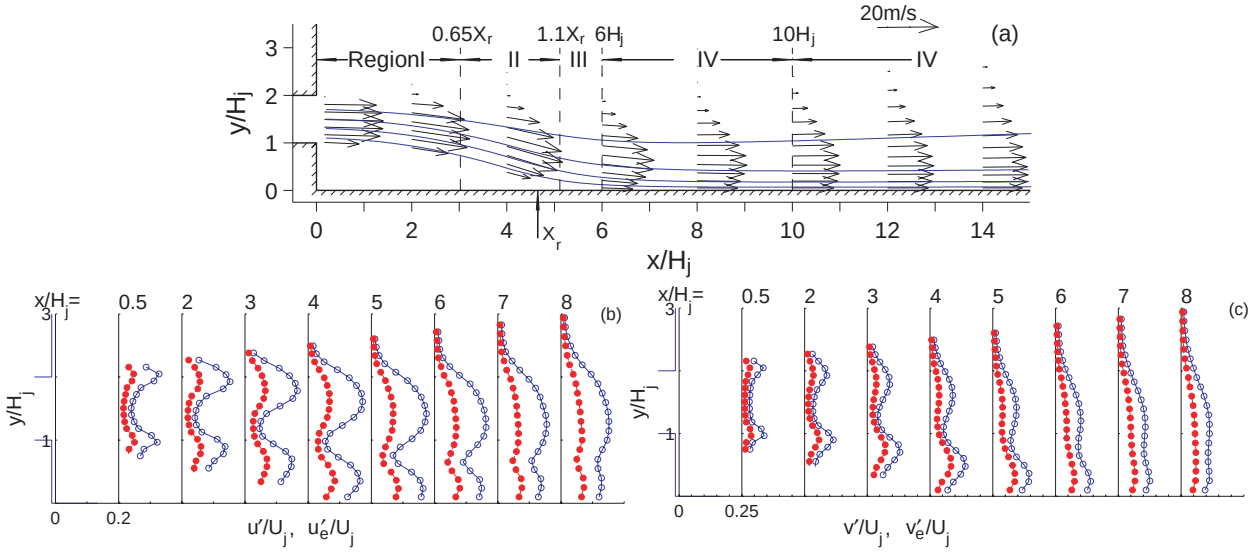

Figure 2. Distributions of (a) vectors of the mean velocity and comparison of the (open symbols) measured and (solid symbols) estimated rms values of (b) the streamwise fluctuating velocities (u' and u'_e) and (c) the vertical fluctuating velocities (v' and v'_e) for offset jet $H_s/H_j = 1.0$

field were 30 to 70% of the actual field. The difference between the measured and estimated rms values was smaller for the vertical fluctuating velocity, suggesting the estimation technique works better for the vertical fluctuations. The estimation process captured fluctuations in both inner and outer shear layers.

The spectra of the fluctuating wall pressure, the fluctuating velocities in the inner and outer shear layer and the estimated velocities at the same location are shown in Fig. 3. The magnitude of the pressure fluctuations and the fluctuations in the inner shear layer grew as the flow evolved downstream and reached a maximum near the reattachment location. The spectrum at this location was broad indicating fluctuating energy in the flow near the wall was distributed in a broad range of frequencies ($fX_r/U_j = 0.2$ to 1.4). As the flow evolved further downstream, another peak emerged with a frequency of $fH_j/U_j = 0.04$ to 0.13 that was associated with the motions form the wall jet structures. More detailed spectral measurements were given in Gao and Ewing.[4] The shape of the estimated spectra were similar to the measured spectra and the characteristic frequency of the estimated and measured spectra occurred at a similar frequency indicating the estimation captured the key structures in the flow. The magnitude of the estimated spectra were less than the measured spectra. The differences in the magnitude varied at different locations caused by the differences in the coherence between the pressure and velocities.

The time series of the measured and the estimated vertical fluctuating velocities, v and v_e, at one location are shown in Fig. 4. The data showed that the measured and the estimated velocities are in reasonable agreement. The low frequency fluctuations which were the key features of the measured signal were captured by the estimation. The amplitude of the fluctuations in the estimated velocities was smaller than that in the measured velocities. There were some high frequency fluctuations that the estimation did not capture.

The dynamics of the fluctuations in the flow were examined by applying a wavelet transform to the fluctuating wall pressure, i.e.,

$$P(a,\tau) = \frac{1}{\sqrt{a}} \int_{-\infty}^{\infty} p(t)\psi^* \left(\frac{t-\tau}{a}\right) dt, \tag{8}$$

where a is the scale of the wavelet, τ is the time translation parameter, ψ is the Morlet wavelet given by

$$\psi(x) = e^{-x^2/2} e^{i5x}. \tag{9}$$

The modulus of the real part of the wavelet coefficient is considered here following Hall and Ewing[7] because it shows both the amplitude of the coefficient and the phase. The results for the pressure at $x/H_j = 3$ to 7 are shown in Fig. 5. The time scale a was converted to frequency using $f = 3.4 \times 10^6/af_s$, where f_s is the sampling frequency. The horizontal dash lines reflect the different frequency ranges observed in

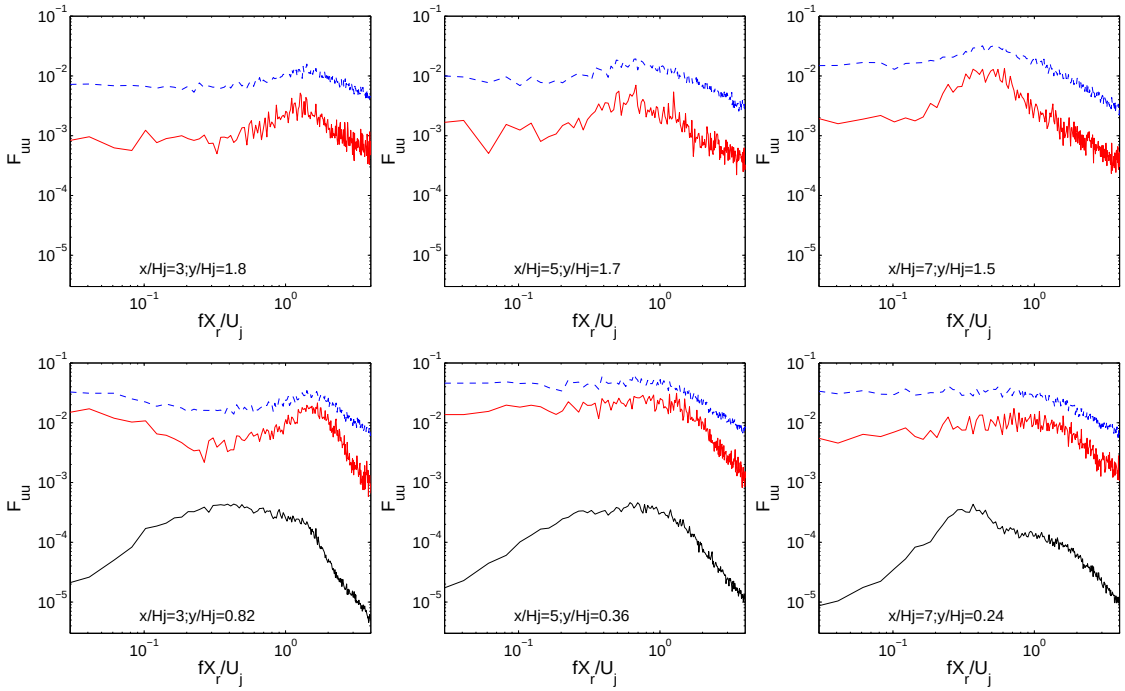

Figure 3. Comparison of the measured wall pressure spectra F_{pp} (black solid line), the measured F_{vv} (dash line) and estimated spectra $F_{v_e v_e}$ (red solid line) of the vertical fluctuating velocity for offset jet $H_s/H_j = 1.0$ at $x/H_j = 3, 5, 7$

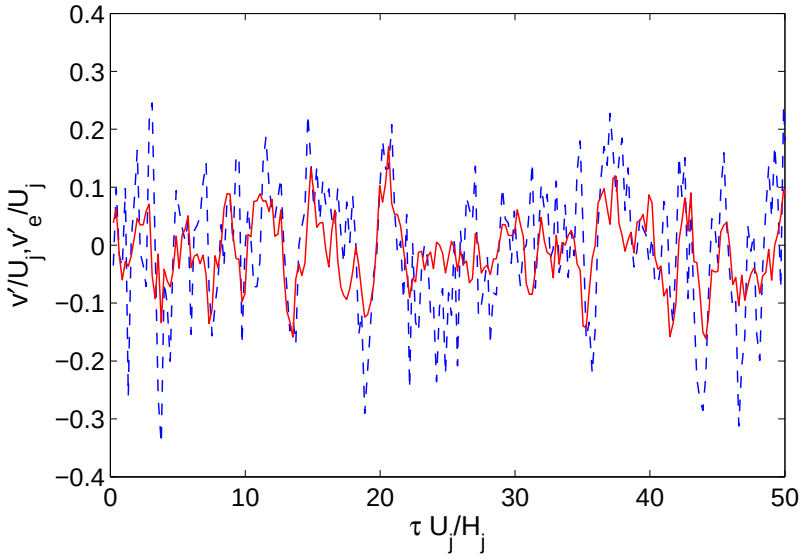

Figure 4. Comparison of the measured transient fluctuating velocity v (dash line) and estimated velocity v_e (solid line) for offset jet $H_s/H_j = 1.0$ at $x/H_j = 3$ and $y/H_j = 0.82$.

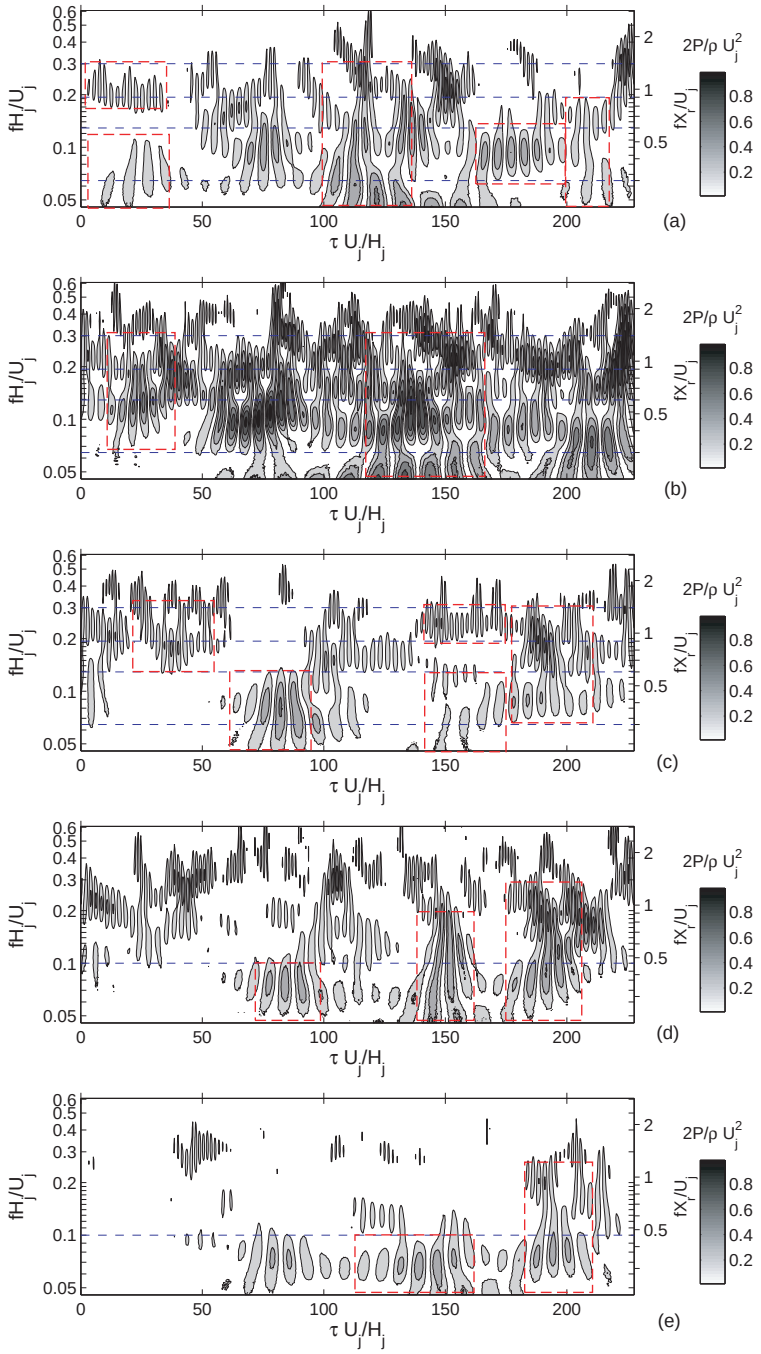

Figure 5. Modulus of the real part of the wavelet coefficients for the fluctuating wall pressure at $x/H_j =$ (a)3, (b)4, (c)5, (d)6 and (e)7 for the offset jet with $Hs/Hj = 1.0$.

Gao and Ewing.[5] The results show that the fluctuations roughly fall into these ranges. The results also show evidence that there is significant variation in the behavior of the fluctuating pressure, particularly near the reattachment region ($x/H_j \leq 5$). For example, the wavelet coefficients for the pressure at $x/H_j = 3$ showed evidence of motions that contribute in all four ranges during the period $100 \leq \tau U_j/H_j \leq 140$, while there was only large coefficient for $0.3 < fX_r/U_j \leq 0.6$ during $170 \leq \tau U_j/H_j \leq 200$. During $0 \leq \tau U_j/H_j \leq 40$, the motions include a weak flapping motion ($fX_r/U_j \leq 0.3$) and shear layer motions with $0.9 < fX_r/U_j \leq 1.4$ and during $200 \leq \tau U_j/H_j \leq 220$, the motions include a weak flapping and contributions from shear layer motions with $0.6 < fX_r/U_j \leq 1.4$. The behavior at other locations varied with time. The high frequency motions were large at $x/H_j = 4$ and gradually decreased at $x/H_j \geq 5$ after the jet attached to the wall. There are evidence of fluctuations convected downstream, particularly the motions in the range $0.3 < fX_r/U_j \leq 0.6$.

The dynamics of the flow structures in the inner shear layer and those formed the wall jet were examined by applying box filters to the estimated velocities. The frequencies of these filters were the characteristic frequencies of the four motions proposed in Gao and Ewing[5] ($fX_r/U_j \leq 0.3$, $0.3 < fX_r/U_j \leq 0.6$, $0.6 < fX_r/U_j \leq 0.9$, and $0.9 < fX_r/U_j \leq 1.4$). The estimated Fourier coefficients for the velocities $\hat{u}_e(x, y, f)$ and $\hat{v}_e(x, y, f)$ were set to zero for frequencies outside of the box filter's range. The streamlines of the filtered fluctuating velocities field at $x/H_j = 3$,4 and 5, viewed from a reference frame travelling at the convection velocity were shown in Fig. 6. The convection velocity of the motions, U_c, was determined here from change in the phase of the cross spectra between the fluctuating wall pressure and the fluctuation velocity at that frequency f with downstream position in Gao and Ewing.[5] The convection velocities in the region $2 \leq x/H_j \leq 8$ were $0.3U_o$ to $0.65U_o$ for the flow structures with frequencies of $fX_r/U_j = 0.3$ to 1.4. The convection velocity from the estimated velocity field will be examined in the future.

The streamlines of the velocity field filtered using the low frequency filter ($fX_r/U_j \leq 0.3$) showed the jet underwent vertical motions near the wall for $y/H_j < 1$, consistent with a flapping motion. The streamlines of the velocity field for the higher frequency ranges showed two rows of counter-rotating large scale flow structures. The lower row structures rotated in the clockwise direction. The locations of these structures coincided with the locations of the shear layer suggested by the rms value of the fluctuating velocities. Both rows approached wall in the region $x/H_j = 3$ to 5. The lower row structure decreased in size while interacting with the wall. The results agreed with the correlation measurements by Gao and Ewing[4] and the cross spectra measurements by Gao and Ewing.[5]

The nature of the periodic motions was examined further using the vorticity estimated by

$$\omega_z = \frac{\partial v_e}{\partial x} - \frac{\partial u_e}{\partial y} \approx \frac{\Delta v_e}{\Delta x} - \frac{\Delta u_e}{\Delta y}, \tag{10}$$

where Δx was approximated using $\Delta x = -U_c \Delta t$. Here, Δt is the time interval, which is 1 over the sampling frequency, and U_c is the convection velocity of the periodic motions. The vorticity of the filtered estimated velocities field at $x/H_j = 3$,4 and 5 are shown in Fig. 7. One component of the mean vorticity was included, so the vorticity in the upper part of the jet was positive and the lower part negative. The vorticity computed using the estimated velocity with box filters for time $100 \leq \tau U_j/H_j \leq 140$ and $170 \leq \tau U_j/H_j \leq 210$ are shown in Fig. 8. The wavelet coefficients were different for the two periods. There was energy in all frequency ranges at $100 \leq \tau U_j/H_j \leq 140$ but only for $0.3 < fX_r/U_j \leq 0.9$ at $170 \leq \tau U_j/H_j \leq 210$. The vorticity showed that the behavior of the jet was indeed different. The jet at $170 \leq \tau U_j/H_j \leq 210$ lacked the low frequency flapping motion and the two inner shear layer motions were also weak. The spatial distributions of vorticity for time $114 \leq \tau U_j/H_j \leq 121$ and $197 \leq \tau U_j/H_j \leq 204$ are shown in Fig. 9. The vorticity shown here were computed using estimated velocity filtered with $fX_r/U_j \leq 1.4$. Large scale structures clearly formed in the inner shear layer and propagate downstream during the period $197 \leq \tau U_j/H_j \leq 204$. The formations of large scale structures in the inner shear layer were not as clear during $114 \leq \tau U_j/H_j \leq 121$. The implications of these differences require further investigation.

IV. Concluding Remarks

Large scale flow structures in an offset attaching jet with an offset height equal to the jet height ($H_s/H_j = 1$) and $Re = 44\,000$ were studied using realizations of the velocity field estimated from simultaneous measurements of the fluctuating wall pressure along the streamwise direction. The modulus of the wavelet coefficient of the fluctuating wall pressure showed evidence that the behavior of the jet changed

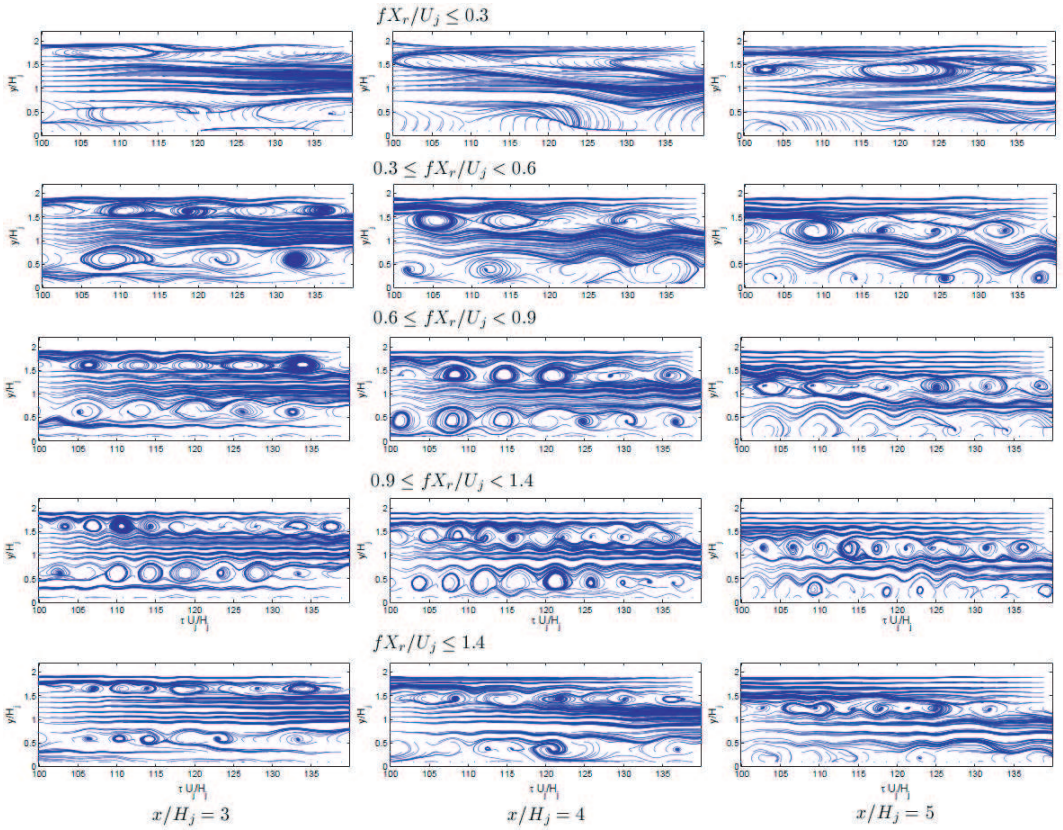

Figure 6. Streamlines of the estimated fluctuating velocity with different filters at x/H_j =3, 4 and 5, viewed from a moving frame with the mean propagation velocity for that frequency.

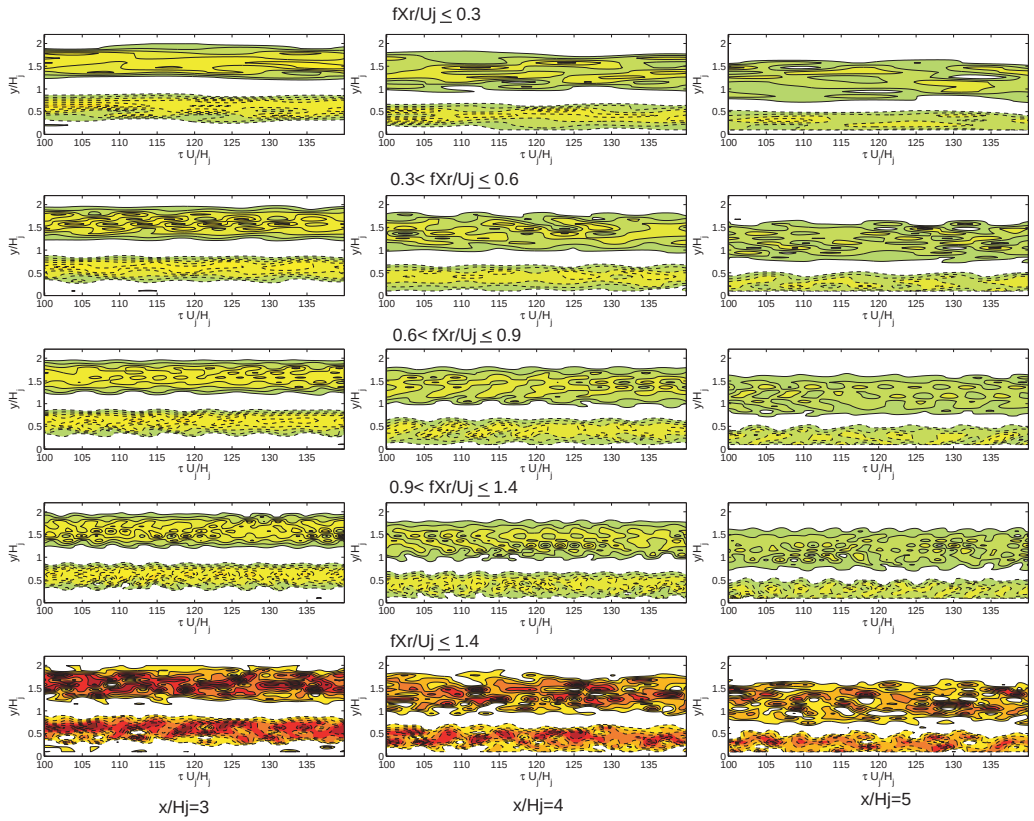

Figure 7. Vorticity computed using the estimated velocity, $(\partial v_e/\partial x - \partial u_e/\partial y - \partial U/\partial y)H_j/U_j$, with different filters at x/H_j =3, 4 and 5. The cutoff level is ±0.5, contour interval is 0.3. Solid lines denote positive vorticity, dash lines denote negative vorticity.

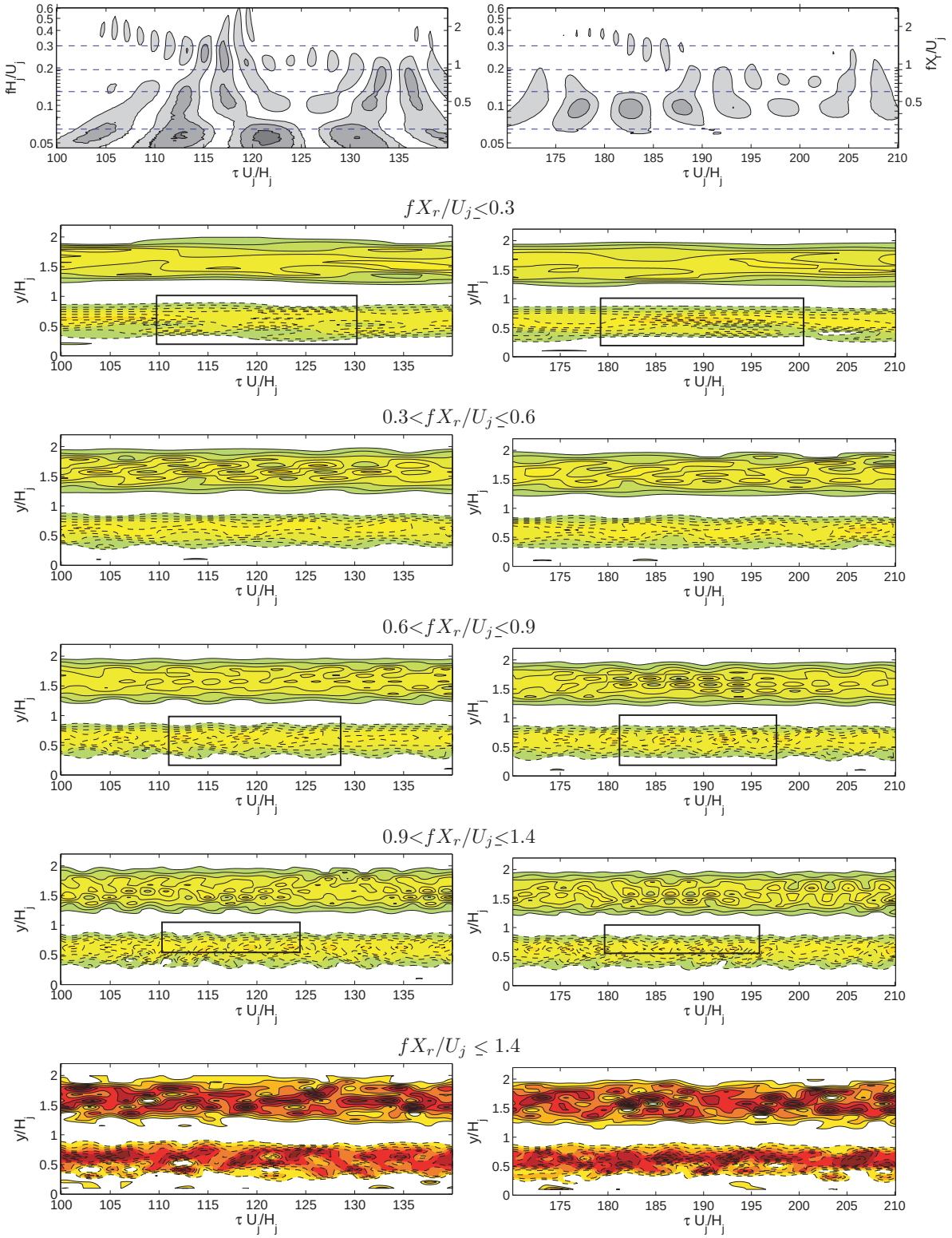

Figure 8. Modulus of the real part of the wavelet coefficient of fluctuating wall pressure and vorticity of the estimated velocity, $(\partial v_e/\partial x - \partial u_e/\partial y - \partial U/\partial y)H_j/U_j$, with different filters at x/H_j =3 for (left) $100 \leq \tau U_j/H_j \leq 140$ and (right) $170 \leq \tau U_j/H_j \leq 210$. The cutoff level is ±0.5, contour interval is 0.3. Solid lines denote positive vorticity, dash lines denote negative vorticity.

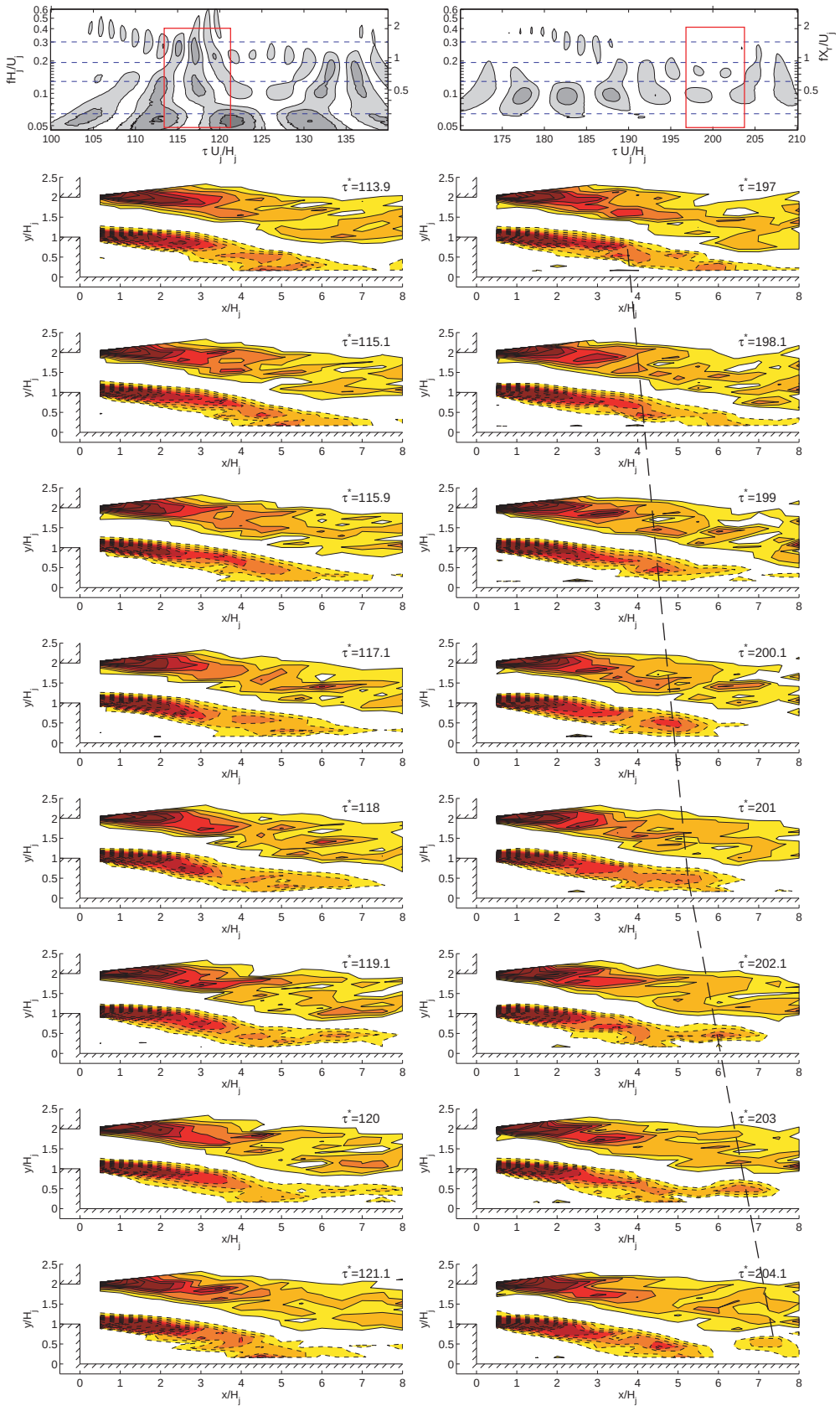

Figure 9. Modulus of the real part of the wavelet coefficient of fluctuating wall pressure at $x/H_j = 3$ and vorticity of the estimated velocity, $(\partial v_e/\partial x - \partial u_e/\partial y - \partial U/\partial y)H_j/U_j$, with a filter $fX_r/U_j \leq 1.4$ for (left) $114 \leq \tau U_j/H_j \leq 121$ and (right) $197 \leq \tau U_j/H_j \leq 204$. The cutoff level is ± 0.5, contour interval is 0.3. Solid lines denote positive vorticity, dash lines denote negative vorticity.

significantly with time. The fluctuations below the attaching jet did seem to fall into different ranges proposed in Gao and Ewing,[5] flapping motions with a frequency of $fX_r/U_j \leq 0.3$, motions that eventually form the wall jet structures ($0.3 < fX_r/U_j \leq 0.6$), the inner shear layer structures with $0.6 < fX_r/U_j \leq 0.9$ and $0.9 < fX_r/U_j \leq 1.4$. The behavior of the jet could include all these four motions or the combinations of motions in different ranges. The estimations of the velocity field during the different periods showed that the behavior of the structures in the jet indeed appeared different. The role of the different motions in these behaviors and the implications of these different behaviors will be studied in future investigations.

V. Acknowledgements

The first author wish to acknowledge the support of Natural Science Foundation of China(10802102).

References

[1]Bruun, H.H., "Hot-wire Anemometry", Oxford University Press, Oxford, 1995

[2]Cherry, N., Hillier, R. and Latour, M. "Unsteady measurements in a separated and reattaching flow." J. Fluid Mech., 144, 13–46, 1984.

[3]Ewing, D. and Citriniti, J., "Examination of a LSE/POD complementary technique using single and multitime information in the axisymmetric shear layer", IUTAM Symp. on Simulation and Identification of Organized Structure in Flows, Eds. J. Sorensen and E. J. Hopfinger and N. Aubry, Lyngby, Denmark, Kluwer Academic Publishers, pp.25-29, 1997.

[4]Gao, N. and Ewing, D., "Experimental investigation of planar offset attaching jets with small offset distances", Exp. in Fluids, 42, pp.941-954, 2007

[5]Gao, N. and Ewing, D., "On the phase velocities of the motions in an offset attaching planar jet", J. Turbulence, 9, No.27, pp.1-21, 2008

[6]Hall, J.W. and Ewing, D., "A combined spatial and temporal decomposition of the coherent structures in the three-dimensional wall jet", AIAA Paper 2006-0308, Reno, NV, 2006

[7]Hall, J.W. and Ewing, D., "The asymmetry of the large-scale structures in turbulent three-dimensional wall jets exiting long rectangular channels", J. Fluids Engr., 129, pp.929-941, 2007

[8]Heenan, A.F. and Morrison, J.F., "Passive control of pressure fluctuations generated by separated flow", AIAA J., 36, pp.1014-1022, 1998

[9]Hudy, L., Naguiba, A. and Humphreys, W. "Wall-pressure-array measurements beneath a separating/reattaching flow region." Phys. Fluids, 15, pp. 706–717, 2003.

[10]Lee, I. and Sung, J., "Multiple-arrayed pressure measurements for investigation of the unsteady flow structure of a reattaching shear layer", J. Fluid Mech., 463, pp.377-402, 2002

[11]Pope, S., "Turbulent Flows", Cambridge University Press, Cambridge, 2000

[12]Tinney, C., Coiffet, F., Delville, J., Hall, A., Jordan P., and Glauser, M., " On spectral linear stochatistic estimation", Exp. in Fluids, 41, pp.763-775, 2006.